Clim Dyn (2012) 39:811–826
DOI 10.1007/s00382-011-1254-3

The effect of Arabian Sea optical properties on SST biases and the South Asian summer monsoon in a coupled GCM

A. G. Turner · M. Joshi · E. S. Robertson · S. J. Woolnough

Received: 12 April 2011 / Accepted: 23 November 2011 / Published online: 11 December 2011

Abstract This study examines the effect of seasonally varying chlorophyll on the climate of the Arabian Sea and South Asian monsoon. The effect of such seasonality on the radiative properties of the upper ocean is often a missing process in coupled general circulation models and its large amplitude in the region makes it a pertinent choice for study to determine any impact on systematic biases in the mean and seasonality of the Arabian Sea. In this study we examine the effects of incorporating a seasonal cycle in chlorophyll due to phytoplankton blooms in the UK Met Office coupled atmosphere-ocean GCM HadCM3. This is achieved by performing experiments in which the optical properties of water in the Arabian Sea—a key signal of the semi-annual cycle of phytoplankton blooms in the region—are calculated from a chlorophyll climatology derived from Sea-viewing Wide Field-of-View Sensor (SeaWiFS) data. The SeaWiFS chlorophyll is prescribed in annual mean and seasonally-varying experiments. In response to the chlorophyll bloom in late spring, biases in mixed layer depth are reduced by up to 50% and the surface is warmed, leading to increases in monsoon rainfall during the onset period. However when the monsoons are fully established in boreal winter and summer and there are strong surface winds and a deep mixed layer, biases in the mixed layer depth are reduced but the surface undergoes cooling. The seasonality of the response of SST to chlorophyll is found to depend on the relative depth of the mixed layer to that of the anomalous penetration depth of solar fluxes. Thus the inclusion of the effects of chlorophyll on radiative properties of the upper ocean acts to reduce biases in mixed layer depth and increase seasonality in SST.

Keywords Arabian Sea · Monsoon · Chlorophyll · Model bias · Mixed layer · South Asia

A. G. Turner (✉) · M. Joshi · E. S. Robertson · S. J. Woolnough
NCAS-Climate, Walker Institute for Climate System Research, Department of Meteorology, University of Reading, Reading RG6 6BB, UK
e-mail: a.g.turner@reading.ac.uk

1 Introduction

Winds in the northern Indian Ocean undergo one of the largest seasonal cycles on the planet thanks to the Asian monsoons during boreal summer and winter. In summer, south–westerly monsoon winds provide India with around 80% (~850 mm) of its annual rainfall, while north–easterly winds bring predominantly dry air across the Arabian Sea in winter. The ability to simulate and predict the timing, duration and intensity of the monsoons is vital for agriculture and other water resource users such as industry. The large seasonality in monsoon winds across the Arabian Sea is strongly coupled with the underlying ocean. As demonstrated in Ju and Slingo (1995) Figure 15, sea surface temperatures (SST) reach around 29.5°C under clear-sky conditions in May. This maximum subsequently falls to around 27°C following the rapid onset of the monsoon winds, almost as low as in boreal winter. As Ju and Slingo (1995) describe, this onset brings strong coastal upwelling off Somalia, as well as enhanced evaporation and ocean mixing. As the monsoon begins to wane, solar heating once again warms the region prior to the autumn equinox. Comprehensive studies such as Schott and McCreary (2001) also describe in detail the complex seasonal cycle of ocean currents in the region, such as the Somali current, which we shall not discuss here.

While many coupled general circulation models (GCMs) can capture the basic seasonality of the monsoons, there are clear biases in the Arabian Sea in the Third Coupled Model Intercomparison Project (CMIP3) models (Meehl et al. 2007). Marathayil et al. (2011) have shown these to consist of cold biases in the northern and central Arabian Sea (of order 2–3°C) during boreal winter and spring, concurrent with excessive north–easterly monsoon winds, mixed layers that are too deep in the north, and enhanced low-level convergence over the west equatorial Indian Ocean. Ju and Slingo (1995) selected anomalous monsoon seasons using a dynamical index and suggested that the surface of the Arabian Sea may act passively, as a regulator, to weakened monsoon flow. After the onset of dynamically strong monsoons, they show reduced Arabian Sea SST for the remainder of the season. Via Clausius-Clapeyron, this could yield reduced moisture transport to India, constraining rainfall variability on interannual timescales. (The interannual variability in monsoon rainfall is surprisingly low at around 85 mm, 10% of the seasonal total.) Some studies have considered the importance of Arabian Sea SST to monsoon rainfall at particular locations over India. In particular, Izumo et al. (2008) found that upwelling-related changes in SST along the Oman and Somali coasts led to variability in rainfall over the Western Ghats (near the west coast of India), with reduced upwelling leading to higher SST and increased moisture transport to the region. Reductions in this upwelling were themselves related to anomalously weak south–westerlies in late spring, caused by high SST in the Seychelles-Chagos thermocline ridge region. Vecchi and Harrison (2004) also showed a relationship in observations between anomalously cold SST in the western Arabian Sea and reduced rainfall in June and July along the Western Ghats.

More generally, summer monsoon area-average rainfall can be shown to have a clear relationship with moisture advected across the Arabian Sea. Using European Centre for Medium Range Weather Forecasts (ECMWF) 40-year Reanalysis (ERA-40) vertically integrated moisture flux and India Meteorological Department (IMD) 1°-gridded rainfall data for the 1958–2001 period, Fig. 1 shows the composite difference between strong and weak monsoon summers (June to September) based on the All India Rainfall index. The figure shows clear evidence of enhanced moisture advection across the Arabian Sea reminiscent of the Somali jet in the lower troposphere, during strong monsoon summers. This coincides with enhanced precipitation over the Western Ghats. The south–westerly moisture flux anomaly turns cyclonically around the monsoon trough leading to enhanced precipitation over central/northern India. Thus conditions over the Arabian Sea are clearly important for monsoon rainfall.

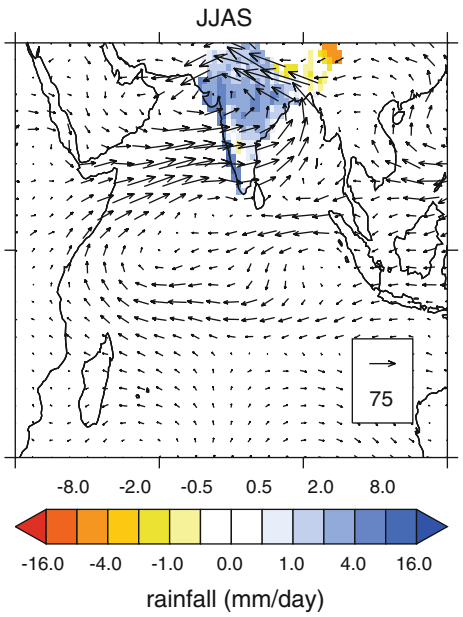

Fig. 1 Composite difference of vertically integrated moisture fluxes from ERA-40 (vectors) and IMD 1°-gridded Indian precipitation (*shading*) for strong minus weak monsoon years, for 1958–2001. The All-India rainfall area-averaged index is used to compute this difference, using a $\pm$ 1 σ threshold. Units are mm/day for rainfall and the unit vector for moisture flux is 75 kg m^{-1} s^{-1}

Given the large seasonal cycle in SST, surface winds and mixed layer depth, the Arabian Sea undergoes a large seasonal cycle in chlorophyll owing to phytoplankton blooms. Furthermore, given that the forcing is semi-annual (monsoonal), two seasonal blooms occur. As the initial review in Lévy et al. (2007) describes, these regular sign changes in vertical mixing and upwelling affect the provision of nutrients at the surface. Based on the assumption that bloom onset occurs owing to physical processes, Lévy et al. (2007) performed a spatio-temporal comparison of bloom onsets (as measured by surface chlorophyll data from the Sea-viewing Wide Field-of-View Sensor (SeaWiFS) platform) with physical processes in the high resolution NEMO ocean GCM. The regional diversity of processes (coastal upwelling; interior upwelling; vertical mixing; horizontal advection) even within the Arabian Sea leads to dramatic contrasts in the timing and intensity of phytoplankton blooms in the region. Lévy et al. (2007) showed seasonal variations in chlorophyll concentrations at various locations in the Indian Ocean based on the SeaWiFS chlorophyll climatology and we reproduce this here, from their data, in Fig. 2 (this version has been calculated on the 1.25° resolution grid of the HadCM3 ocean model; see Sect. 2 for details). Clear evidence of a semi-annual cycle in concentration can be seen in the western (Somali coast) and central Arabian Sea regions (marked A and B respectively). For the central Arabian Sea (the

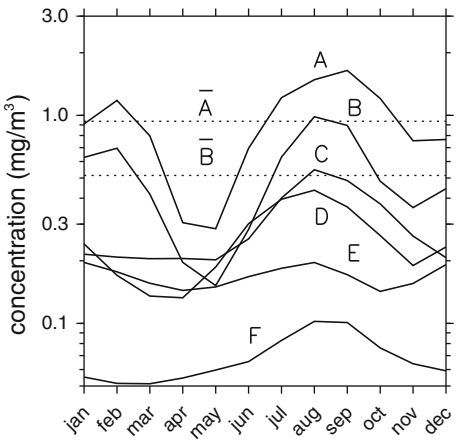

Fig. 2 Annual cycle of chlorophyll concentrations derived from the monthly 1.25° resolution SeaWiFS climatology supplied to the ocean model, derived from the data at http://www.nio.org. The regions *A–F* are chosen to approximately match those in Figs. 1 and 2 of Lévy et al. (2007). *A*: western Arabian Sea (60°E, 19°N; the main upwelling region), *B*: central Arabian Sea (66°E, 15°N). *C*: Lakshadweep Sea (73°E, 10°N; west of Kerala), *D*: southwest Bay of Bengal (85°E, 9°N), *E*: central Bay of Bengal (90°E, 14°N), and *F*: south central Indian Ocean (75°E, 21°S). Annual mean values are indicated by *horizontal lines* for the *A* and *B* stations only

largest summer bloom area), Lévy et al. (2007) show mixed layer processes to be fundamental in driving the summer bloom onset: rapid deepening of the mixed layer leading to mixing of nutrients to the surface and phytoplankton blooming. Horizontal advection also brings in nutrient-rich waters from the adjacent coastal upwelling region. For the main winter blooms over the north–east and north–west Arabian Sea, Lévy et al. (2007) also showed mixed layer processes rather than upwelling to be the cause.

The seasonality in chlorophyll near the ocean surface can perturb the penetration of solar fluxes into the upper ocean and hence its vertical temperature profile. Such perturbations to the temperature profile of the Arabian Sea could potentially alter conditions at the surface, ultimately impacting on SST and the supply of moisture to the monsoon. Seasonally varying chlorophyll is an example of a missing biogeochemical process that is only recently beginning to be implemented in the latest Earth System models. Historically, coupled ocean-atmosphere GCMs such as HadCM3 controlled the radiative properties of the ocean via solar attenuation rates, such as the penetration curves at red and blue wavelengths fitted by Paulson and Simpson (1977) to various Jerlov water types (Jerlov 1968). These curves feature assigned length scales (ζ_i) associated with exponential decay for the transmission of light at depth z in each of the wavelength bands ($I = I_0 \exp^{-z/\zeta_i}$ for bands i = 1, 2). For Jerlov Type 1B (approximating clear water) they suggest decay scales of 1 and 17 m for red and blue wavelengths respectively, while for Jerlov Type III (more turbid waters perhaps associated with high chlorophyll concentrations) they suggest 1.4 and 7.9 m respectively. Thus they demonstrated much weaker penetration at the blue end of the spectrum in more turbid waters. GCMs typically feature a uniform water type throughout the ocean. Moving beyond this simple method, the effects of chlorophyll on the radiative properties of the ocean can be determined empirically and hence incorporated into GCMs. For example, Ohlmann (2003) examined penetration depth scales associated with chlorophyll concentrations and outlined a pair of exponential equations suitable for chlorophyll-dependent solar transmission. Such a chlorophyll-dependent radiation scheme has already been demonstrated in a study of the tropical Pacific Ocean in experiments with the LICOM coupled model (Lin et al. 2007).

In an early study, Sathyendranath et al. (1991) used remotely sensed information on ocean colour and a 1D model to suggest the importance of chlorophyll for controlling SST and atmosphere-ocean interactions, motivating more detailed study. Some studies have examined the impact of chlorophyll on the Arabian Sea in a variety of GCM component models. Nakamoto et al. (2000) used satellite-derived chlorophyll to drive the OPYC ocean GCM (OGCM) and showed amplification of the seasonal cycle at 20°N. This consisted of slight cooling during the summer and winter monsoon seasons and warming during the inter-monsoon periods. To determine possible effects of chlorophyll-forced SST changes on the atmosphere, Shell et al. (2003) forced the CCM3 atmosphere-only GCM (AGCM) with SSTs derived from an OGCM, themselves generated by applying chlorophyll perturbations globally. In their study, very small changes to July precipitation in India were noted, although a general increase in tropical convection was found in the summer hemisphere due to near-surface warming. However, we reiterate the importance of coupled feedbacks in the Arabian Sea to its climate and to the monsoon, as described earlier in this introduction. Wetzel et al. (2006) were among the first to perform a fully coupled global study, also incorporating a biogeochemical model to determine solar attenuation rates. In addition to the impacts on ENSO such as a reduction in variability, their brief examination of the Arabian Sea at 20°N reveals an improvement in the seasonal cycle of SST, with the largest difference found in autumn with a chlorophyll-induced warming of over 1°C in the west. For the summer monsoon (defined therein as July to September), increases in rainfall of around 3 mm/day were noted. Finally, Gnanadesikan and Anderson (2009) used a coupled GCM forced with satellite chlorophyll to show annual mean cooling of between 0.2 and 0.6 K in the Arabian Sea, attributable to the local or remote effects of tropical

chlorophyll concentrations in excess of 0.2 mg m^{-3}, although no effects on the monsoon were noted.

Other studies have examined the effects of chlorophyll on the tropical Pacific, focusing on the equatorial cold tongue region and upwelling in the east. In the OPYC OGCM, Nakamoto et al. (2001) showed additional heating and a shoaled mixed layer that led to increased upwelling further east via interactions with currents. Lin et al. (2007) also noted the enhanced upwelling using the coupled LICOM model. However, Lengaigne et al. (2007) used two different coupled models to show warming of the eastern equatorial Pacific by around 0.5°C, particularly during the main upwelling season, hence damping the seasonal cycle. Lengaigne et al. (2007) and Anderson et al. (2009) both highlighted the importance of the distribution of chlorophyll and Gnanadesikan et al. (2010) show the clear impact of its distribution on the positioning of subtropical cyclones in the northwest Pacific, using the GFDL CM2.1 coupled model. Thus changes in chlorophyll behaviour can have clear implications for atmospheric convection and the ocean mean state at various locations throughout the tropics.

The purpose of this study is to examine the role of local seasonal chlorophyll blooms on the mean climate of the Arabian Sea and determine any impact on the South Asian summer monsoon via changes in Arabian Sea SST. Previous studies have either not used fully coupled ocean-atmosphere models, or have considered the Arabian Sea and its impact on the mean monsoon only briefly. Here we isolate the effect of chlorophyll in the Arabian Sea by looking at first order (its presence) and seasonal considerations.

In Sect. 2 we describe the model and observed datasets used before detailing the experimental design, and in Sect. 3 we compare the model against observations. In Sect. 4 we describe and discuss the results of experiments using SeaWiFS chlorophyll forcing. Finally conclusions are discussed in Sect. 5. We will not consider feedbacks on the biology itself, nor wider biogeochemical feedbacks beyond the scope of this study.

2 Methods

This section describes the model and observed datasets used for comparison and gives details of the experimental design.

2.1 The model

In this study we use the HadCM3 coupled ocean-atmosphere model, consisting of the HadAM3 atmospheric component (Pope et al. 2000) solved on a 3.75° longitude × 2.5° latitude grid on 19 vertical levels and an ocean model at 1.25° resolution in the horizontal on 20 vertical levels (Gordon et al. 2000). This model can be integrated for long periods without the need for flux adjustments to counteract climate drift, since the drift is less than a hundredth of a degree per century (Gordon et al. 2000). Upper ocean resolution is approximately 10 m in the top few layers, and the mixing scheme is based upon the Kraus-Turner formulation (Kraus and Turner 1967). The scheme seeks to balance the energy available for mixing (e.g., via surface winds) with buoyancy anomalies at the ocean surface. Mixing occurs down from the surface until such a depth as no more energy is available for mixing (Foreman 1990): at this point, the mixed layer depth is defined. In the standard version of the model, absorption of solar radiation in the upper ocean is governed by a two-band scheme based on Paulson and Simpson (1977) with approximately clear water in all oceans, although all red wavelengths above a certain cut-off (689 nm) are assumed to be absorbed in the surface layer. Modifications to this scheme as used in the experiments here are discussed in Sect. 2.3.

A distinct advantage of this model over more recent higher resolution models is its relatively cheap computational cost, allowing experiments lasting several decades to be run relatively easily. As we are not expecting the model to reproduce with high fidelity the necessary fine-scale physical processes necessary for producing basin wide variations in chlorophyll (e.g., the structure of upwelling), a chlorophyll climatology shall be imposed directly. Thus the dynamics of the system will not feed back on phytoplankton development. Basic details of the monsoon simulation and its validation against observations will be discussed in Sect. 3.

2.2 Observed data used

Comparisons with observed sea-surface temperature are made with the HadISST dataset (Rayner et al. 2003), originally on a one-degree grid. For atmospheric dynamical fields, the ECMWF ERA-40 re-analysis is used (Uppala et al. 2005) covering the period 1958–2001. Vertically integrated moisture fluxes are calculated between the surface and 100 hPa using these data following:

$$\mathrm{VIMF} = \frac{1}{g} \int_{1{,}000}^{100} \mathbf{u} q \, \mathrm{dp}. \quad (1)$$

For comparisons with observed mixed layer profiles the L'OCEAN monthly climatology prepared by de Boyer Montégut et al. (2004) has been used, comprising around five million profiles of mechanical bathythermograph (MBT)

and Argo data from 1941 to September 2008. These data define the mixed layer depth based on excursions in temperature of 0.2°C from that at 10 m depth, and were obtained from http://www.locean-ipsl.upmc.fr/~cdblod/mld.html.

In Fig. 1, we also used the All-India Rainfall index of seasonal area-mean rainfall for India (Parthasarathy et al. 1994), and daily 1°-gridded rainfall data from IMD (Rajeevan et al. 2006). We use an enhanced version of this dataset (M. Rajeevan, personal communication 2007), comprising 2,140 stations and increased density over the northern plains.

Proxy data for chlorophyll concentrations (in mg m^{-3}) in the ocean mixed layer are taken from the Sea-viewing Wide Field-of-View Sensor (SeaWiFS) data compiled by Lévy et al. (2007) into an eight-daily climatology based on April 1998–March 2005 inputs. Variations associated with the large El Niño of 1997 have been avoided, and Lévy et al. (2007) have interpolated carefully over missing data in the far north Arabian Sea during boreal summer, absent due to cloudiness and dust storms during the period. This climatology, gridded at 0.5° resolution over the Indian Ocean, has been obtained from http://www.nio.org. To incorporate these data into the ocean component of HadCM3 in experiments to be described later, we bi-linearly interpolate to the model resolution of 1.25° and generate a monthly-mean climatology.

Assessing the accuracy of SeaWiFS chlorophyll data in the Arabian Sea is difficult due to the paucity of in situ observed data. In a research cruise south of Gujarat on the west coast of India in November 1999, Desa et al. (2001) suggested that SeaWiFS was overestimating chlorophyll concentrations there due to backscatter from other constituents (perhaps from river discharge). Despite this, Desa et al. (2001) did measure values in the range 0.2–4 mg m^{-3}, consistent with typical values in SeaWiFS. More generally, Gregg and Casey (2004) noted the SeaWiFS product to be more reliable over the open ocean (bottom depths over 200 m, which includes the Arabian Sea away from the coasts). They did caution that Arabian Sea in situ measurements were only available during winter. Conkright and Gregg (2003) noted that SeaWiFS data were also likely to be reliable over the open oceans, being within 10% of blended products constructed from in-situ observations and Coastal Zone Color Scanner data. Finally, in a comparison of SeaWiFS chlorophyll data with retrievals from the MODIS satellite and despite a global mean bias in both datasets, Gregg and Casey (2007) suggested that the poor temporal sampling of the satellite products (biased toward periods free of thick atmospheric aerosol, which also coincide with the highest phytoplankton growth periods) could lead to underestimates in chlorophyll concentrations of up to 30%. This is particularly pertinent to the Arabian Sea region.

2.3 Experimental design

We perform 50-year experiments with HadCM3 under various conditions, in addition to a control integration for comparison.

In the experiments, observed chlorophyll concentrations are read directly into the model. Using empirical relationships fitted by Ohlmann (2003), these concentrations are converted to penetration depth scales and relative weights suitable for implementation in a two-band solar absorption scheme (their Eqns. 6a–d, as also used in Lin et al. 2007). In the first experiment, time-invariant annual mean chlorophyll concentrations are prescribed in the Arabian Sea only, and set to 0.05 mg m^{-3} elsewhere. Using an example high chlorophyll concentration of 1 mg m^{-3}, the relationships fitted by Ohlmann (2003) (reciprocals of their Eqns. 6c, d) yield exponential decay length scales of 1.8 and 7.4 m for red and blue light respectively. This experiment is compared to a control integration (*chl_control*) using 0.05 mg m^{-3} chlorophyll globally and solar penetration determined by the Ohlmann (2003) equations (scales 2.6 and 24.0 m for red and blue wavelengths). Some authors (e.g., Gnanadesikan and Anderson 2009) have used completely clear conditions for their control experiments to determine the full physical impact of chlorophyll, however others (e.g., Shell et al. 2003) use small finite values. In this way, a more realistic evaluation of its impact in the GCM framework can be derived. In a second experiment, the annual cycle of chlorophyll concentrations in the Arabian Sea is read by the model, and linearly interpolated to daily values. The annual cycle of chlorophyll, as determined from the Lévy et al. (2007) climatology and interpolated to the ocean model grid, is shown in Fig. 3. (The annual cycles at various points in these data were earlier shown in Fig. 2.) Note that only those values in the Arabian Sea are considered. Comparison of transmission profiles using the chlorophyll-dependent method of Ohlmann (2003) and the simple water-type scheme of Paulson and Simpson (1977) reveals that at 50 m depth, Jerlov type 1B is roughly equivalent to 0.1–0.3 mg m^{-3}, and type III to 1.0–1.3 mg m^{-3} chlorophyll. Thus the range of observed chlorophyll values in the Arabian Sea (see curves A, B in Fig. 2) is roughly consistent with a transition between clear and turbid water (these two water types). The effect of variations in chlorophyll on surface albedo have been neglected but these are of much smaller magnitude than any projected changes in absorption of solar radiation. A summary of the experiments performed is shown in Table 1.

3 The Arabian Sea and South Asian summer monsoon in HadCM3

The monsoon simulation in HadCM3 has been studied extensively (e.g., Turner et al. 2005, 2007; Turner and

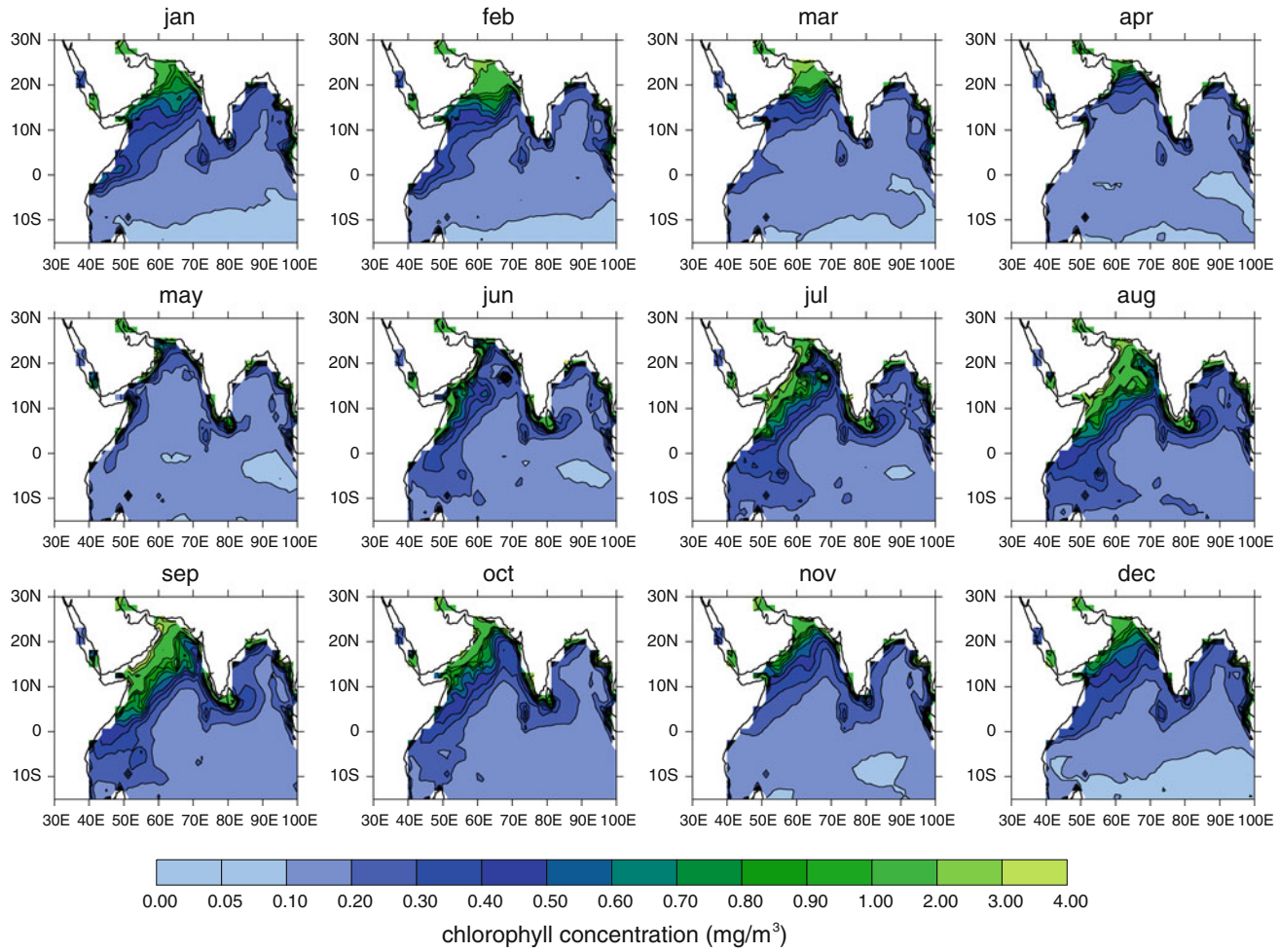

Fig. 3 Monthly spatial variations in the prescribed seasonal cycle of chlorophyll in the SeaWiFS experiments on the 1.25° ocean model grid. Climatology derived from the April 1998–March 2005 data constructed by Lévy et al. (2007)

Table 1 Summary of 50-year experiments performed with HadCM3

Name	Description
chl_control	0.05 mg m^{-3} chlorophyll applied globally
ann_mean	Annual mean SeaWiFS chlorophyll in Arabian Sea
ann_cycle	Varying SeaWiFS chlorophyll in Arabian Sea

Slingo 2009) and inter-model comparisons have shown the seasonal cycle in the broad Asian monsoon rainfall to be among the best of the CMIP3 models (Annamalai et al. 2007). The seasonal cycles of lower and upper tropospheric zonal winds are very close to reanalysis products over the broad domain (Turner et al. 2005). The main biases during summer (JJAS) consist of an excessive Somali jet at low levels (Turner et al. 2005) and a slightly delayed monsoon resulting in weak June rainfall (Turner and Slingo 2009).

A thorough examination of the mean state in HadCM3 will not be carried out here (see Pope et al. 2000; Gordon et al. 2000, for the global picture in addition to earlier studies by the lead author) however Fig. 4 shows boreal winter (DJF) and summer (JJAS) mean conditions in the Indian region for the *chl_control* integration, although this is very similar to the standard version of the model. During boreal summer, HadCM3 well simulates the gross features of the monsoon flow, although it is slightly excessive, especially as it hits northern peninsular India. Into the Bay of Bengal, the meridional component of the flow is slightly weaker than in observations, perhaps reflecting an imperfect response of the Somali jet to orographic forcing around the East African Highlands (Slingo et al. 2005). The summer precipitation structure over the Indian region is rather good: the maximum near the Western Ghats is well simulated considering the horizontal resolution, although the rain shadow over south-east India is too dry. Strong wet biases in the western Indian Ocean just north of the equator are present here and common among current coupled GCMs (Marathayil et al. 2011). Although some of the coastal upwelling off Somalia associated with the monsoon jet is captured, the 1.25° horizontal resolution and

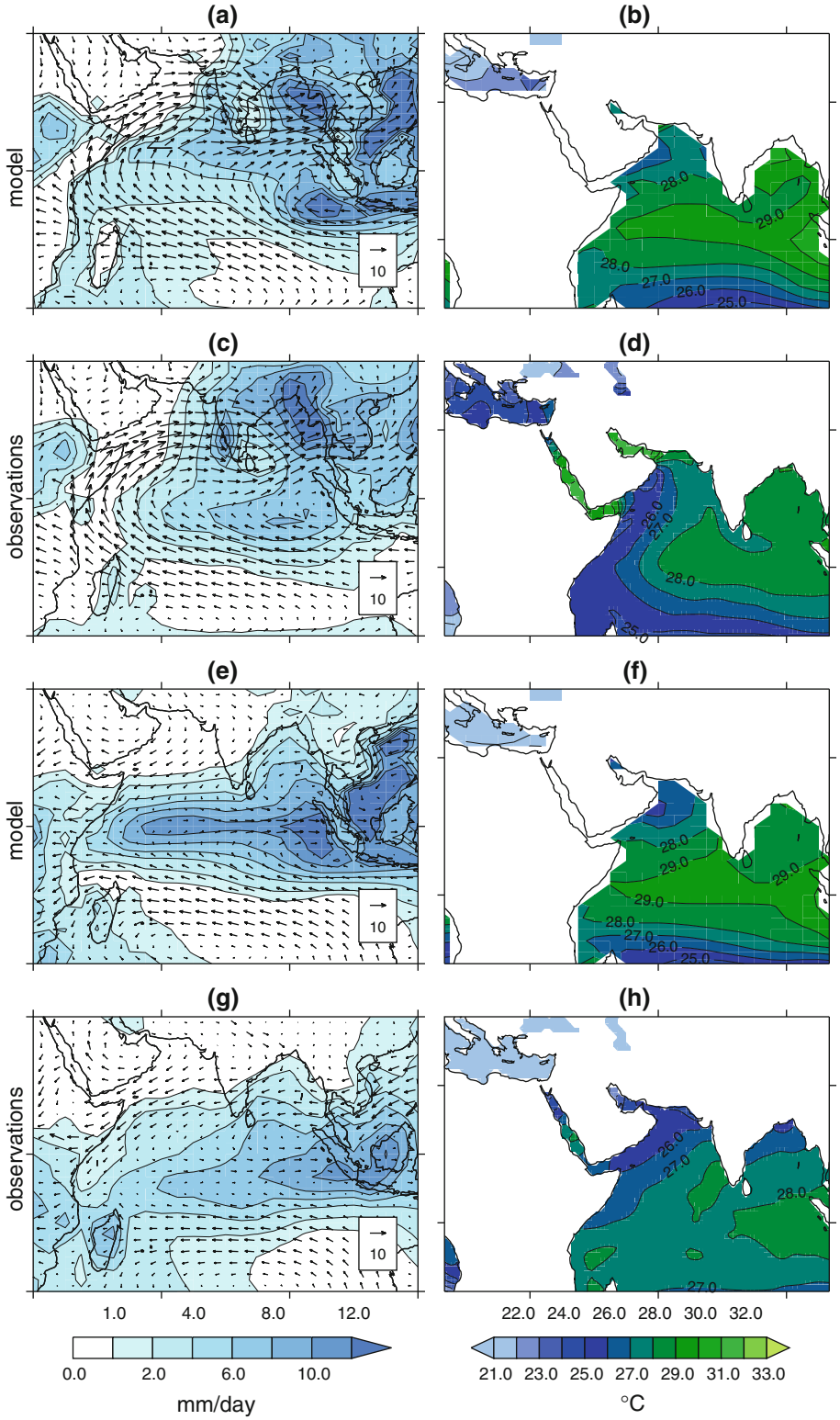

Fig. 4 Seasonal mean lower tropospheric (850 hPa) wind and precipitation (*left*) and SST (*right*) in boreal summer (JJAS; **a**–**d**) and winter (DJF; **e**–**h**) in the 50-year coupled model *chl_control* run (**a**, **b**; **e**, **f**) and observations (**c**, **d**; **g**, **h**). Winds are taken from the ERA-40 reanalysis over 1958–2001. Precipitation is from GPCP (1979−2008) whilst HadISST SSTs are used. Units are ms^{-1}, mm/day and °C

inadequate response of the surface to upwelling mean that much of the western Indian Ocean near the coast is too warm.

In boreal winter (DJF), the precipitation signal again reveals a wet bias in the western Indian Ocean, in addition to over the South China Sea. However the structure is good over the Arabian Sea and Bay of Bengal. At the ocean surface, temperatures are too warm, particularly along the equator, perhaps forcing the precipitation wet bias there. The north-south gradient is correctly simulated in the

Arabian Sea. SST variations though the annual cycle are described later.

We note that particular biases outlined here are unlikely to affect experimental results, as ultimately we are prescribing chlorophyll concentrations, rather than allowing their evolution according to physical processes.

On interannual timescales, variability is too large, as found in Turner et al. (2005). Teleconnections with ENSO are also too weak and mistimed, leading to spring (rather than summer) surface temperatures in the East Pacific correlating most strongly with monsoon rainfall. This bias relates to a poor mean state in the equatorial west-central Pacific in HadCM3, displacing the anomalous diabatic heating and ascent associated with ENSO (Turner et al. 2005). The teleconnection was only simulated well in four CMIP3 coupled GCMs (Annamalai et al. 2007) and will not unduly affect results here, given that the focus is on local processes in long integrations and perturbations are not being made outside of the Arabian Sea region.

4 Results of prescribing chlorophyll concentrations in the Arabian Sea

In this section we describe the results of experiments in which chlorophyll concentrations are prescribed directly using a monthly climatology based on the SeaWiFS data produced for Lévy et al. (2007) and converted to penetrating solar fluxes using the Ohlmann (2003) method as described in Sect. 2. We test the impact of imposing an annual mean chlorophyll concentration on the Arabian Sea (*ann_mean*), and further the impact of the seasonal cycle of chlorophyll (*ann_cycle*) on the climatology of the region and of the Asian monsoon in comparison with the *chl_control* experiment.

4.1 Annual mean SeaWiFS climatology forcing

Here we describe the results of the comparison between applying a fixed annual mean of chlorophyll (*ann_mean*) in the Arabian Sea against the control integration in which chlorophyll is held constant globally at the low value of 0.05 mg m^{-3} (*chl_control*). Results for boreal spring and summer can be seen in Fig. 5. In response to the increased absorption by solar radiation near the surface, the mixed layer is stabilized and hence shoals in all months (Fig. 5a–f). Immediately obvious is the complex spatial structure in the mixed layer depth signal reflecting the large spatial inhomogeneity in chlorophyll concentration described in Figs. 2 and 3. In particular, the shoaling response of the mixed layer is not spread evenly over the Arabian Sea in all months. Statistically significant SST warming occurs over much of the Arabian Sea in April and May and over a smaller region in June (Fig. 5h–j), culminating in increased evaporation and increases in column vertically integrated moisture advected across India and Southeast Asia (Fig. 5n). Enhanced moisture convergence during June leads to significant increases in precipitation (Fig. 5r) strengthening the monsoon onset. During May, moisture fluxes are also enhanced consistent with earlier development of the monsoon. A small region of slight but significant cooling in the western Arabian Sea in July and August (Fig. 5k, l) results in weakened advection of moisture to India and a reduction of August monsoon rainfall by around 1 mm/day over central India, although this change is not statistically significant.

To examine the cause of the changes in early summer moisture flux and monsoon precipitation in more detail, Fig. 6 shows changes in surface latent heat flux and lower tropospheric wind in June and July, months with contrasting precipitation signals. In June, large increases in evaporative flux are found over the Arabian Sea, passing more moisture to the atmosphere; the additional moisture is then advected over India. The increases in SST and latent heat flux are consistent with the atmosphere being forced by the ocean. The low-level monsoon flow is also enhanced by around 1 m s^{-1}, resulting from the stronger meridional temperature gradient in May/June and as a feedback on the enhanced precipitation itself. Thus both winds and evaporative fluxes have contributed to the increase in moisture advected to India. In July, colder SSTs in the west of the Arabian Sea (Fig. 5k) lead to reduced latent heat fluxes at the surface, leaving only a small region of additional moisture by the Indian coast (Fig. 6b).

Significant signals of reduced precipitation in the east equatorial Indian Ocean in June and July (and extending to the west but of smaller magnitude) are consistent with enhanced ascent over the Indian region (e.g., Krishnan et al. 2000) and act to partially ameliorate model precipitation biases shown in Fig. 4. The enhanced ascent over India leads to anomalous subsidence occurring over the equatorial Indian Ocean via the monsoon Hadley circulation (tested using vertical winds at the model level closest to 500 hPa, not shown).

4.2 Seasonally varying SeaWiFS climatology forcing

In the second experiment (*ann_cycle*), we allow the full annual cycle of chlorophyll concentration (Figs. 2 and 3) to be input to the ocean model over the Arabian Sea. The complex spatio-temporal evolution of this field is reflected in the climatological response of the northern Indian Ocean region as seen in Fig. 7. Slightly weaker mixed layer shoaling than in the annual mean case is noted from April to June (Fig. 7b–d). This occurs because the overall

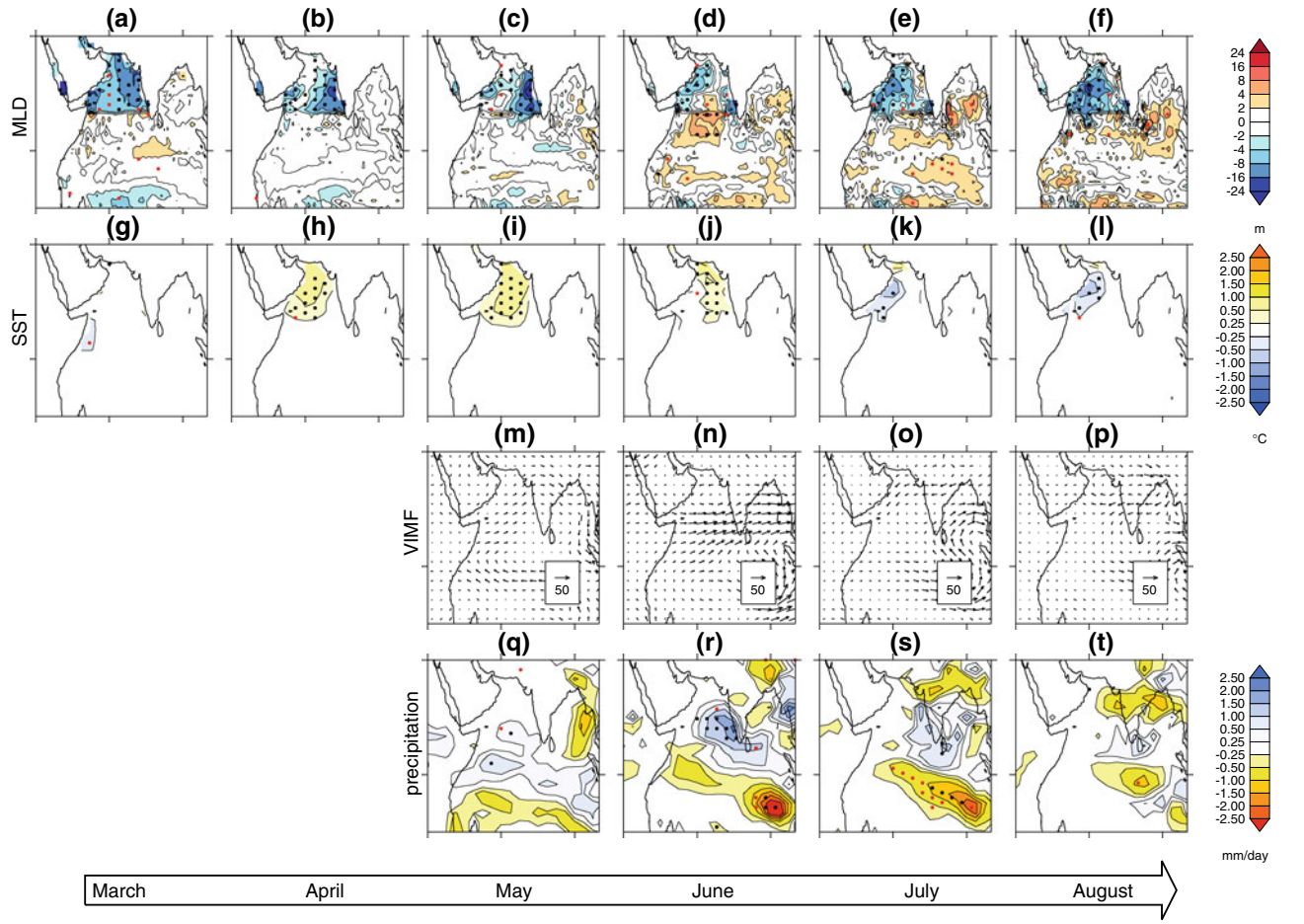

Fig. 5 Spring and summer monthly composite differences between the annual mean SeaWiFS experiment (*ann_mean*) and global chlorophyll control integration (*chl_control*) for mixed layer depth (**a**–**f**), SST (**g**–**l**), vertically integrated moisture flux (**m**–**p**) and precipitation (**q**–**t**). Units are m, °C, kg m^{-1} s^{-1} and mm/day respectively. Months March to August are shown from *left* to *right*, although March/April moisture flux and precipitation *panels* are omitted for clarity as they are well before the rainy season. In the *contoured plots*, differences statistically significant above the 90% (95%) level are shown by *red* (*black*) *stipples*. The unit moisture flux vector is 50 kg m^{-1} s^{-1}

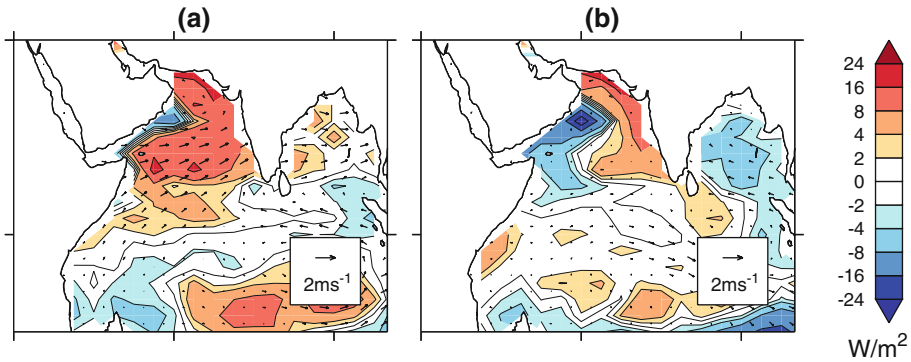

Fig. 6 Early summer monthly composite differences of latent heat flux and lower tropospheric (850 hPa) wind between the *ann_mean* and *chl_control* integrations during (**a**) June and (**b**) July. Units are Wm^{-2} and ms^{-1} respectively

increase in chlorophyll concentration over the 0.05 mg m^{-3} control experiment is less during these months than in the annual mean case for points in the Arabian Sea (compare curves A, B in Fig. 2 with their annual mean counterparts $\overline{A}, \overline{B}$). Following July, increased chlorophyll forcing compared to the annual mean experiment yields only slightly more shoaling owing to the cumulative effects of previous months. In SST, April and May temperature anomalies of up to 0.5°C cover much of the Arabian Sea, reaching 1°C in places (Fig. 7h, i), but these reduce to only

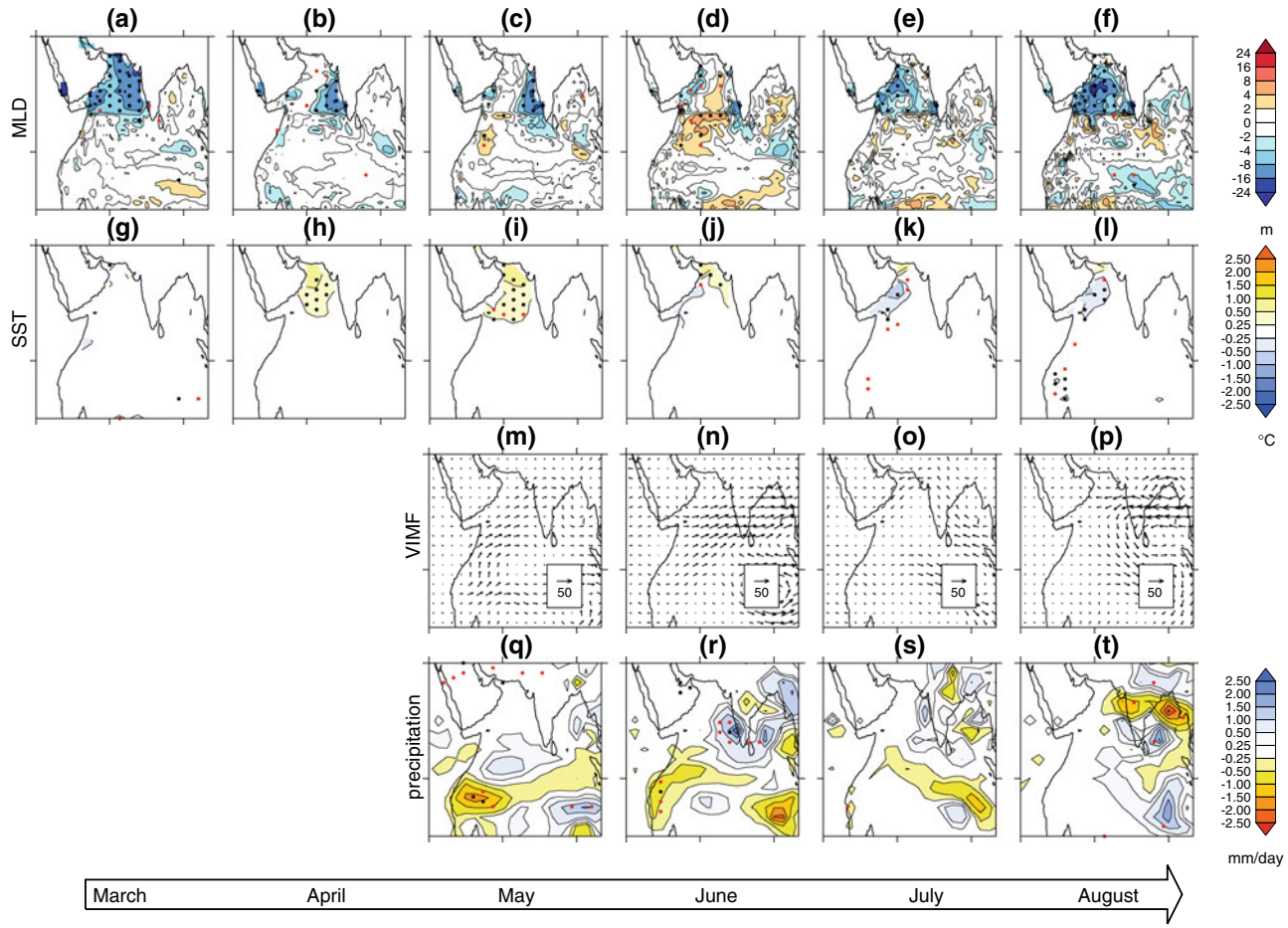

Fig. 7 As in Fig. 5 but for the summer monthly composite difference between the seasonally varying SeaWiFS experiment (*ann_cycle*) and global chlorophyll control integration (*chl_control*)

a small region at the north of the Arabian Sea by June, significant at the 90−95% level. The cumulative effect of increased SST through late spring is one of increased atmospheric moisture, and stronger moisture fluxes incident upon southern India result in precipitation increases over Kerala of up to 2 mm/day in June, significant at the 95% level. The contributions to the enhanced moisture flux from evaporative fluxes and strengthened monsoon flow are similar to those in Fig. 6 for the *ann_mean* experiment (not shown). Changes during the mature monsoon season are consistent with anomalous moisture flux signals and results shown earlier, but are statistically insignificant. We do not see the consistent large increases in rainfall on the west coast of India that Wetzel et al. (2006) noted from July to September, likely due to the different SST response in their study (see later for further details). We have therefore demonstrated that by perturbing the solar absorptive properties of the Arabian Sea in accordance with an observed seasonal cycle of chlorophyll from SeaWiFS data, significant impacts can be found on the monsoon onset and the climate of the Arabian Sea.

We examine the seasonal cycle of SST in the Arabian Sea over the west central region in the SeaWiFS perturbation experiments in Fig. 8. This is calculated over 58−62°E, 15−18°N: chosen as it represents one of the largest regions of chlorophyll and SST variability in the central Arabian Sea, while being some distance from the coast. Most notable are the large biases with respect to observations, particularly the large cold bias in boreal winter and spring, and the warm bias following the monsoon onset, potentially owing to a poor response of upwelling to the Somali jet. Figure 8 shows a clear increase in seasonality from late boreal spring to the monsoon onset in June, with SSTs warmer by up to 0.5°C in the *ann_mean* experiment. Similarly, during boreal winter and summer when the annual cycle in SST recedes, the *ann_mean* and *ann_cycle* experiments show increased reductions in SST. We note that the largest impact on SST is in boreal spring and

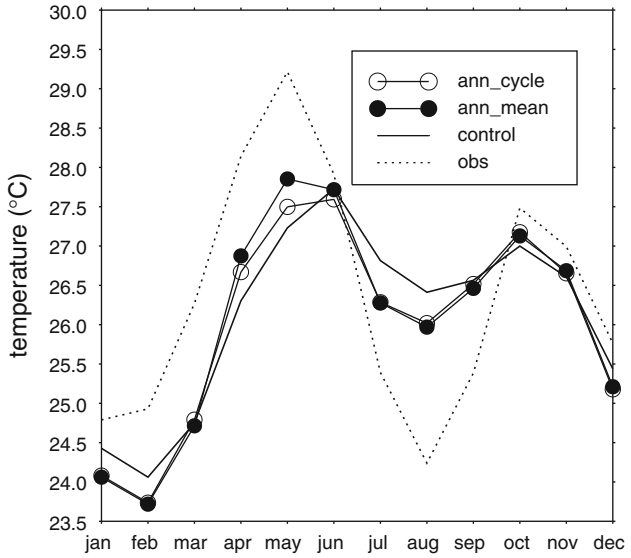

Fig. 8 Mean seasonal cycle of SST in the 58−62°E, 15−18°N region of the west–central Arabian Sea in the *ann_mean* (*solid circle*) and *ann_cycle* (*white circle*) SeaWiFS-forced integrations with the *chl_control* integration (*solid*) and HadISST observations (*dotted*). Units are °C

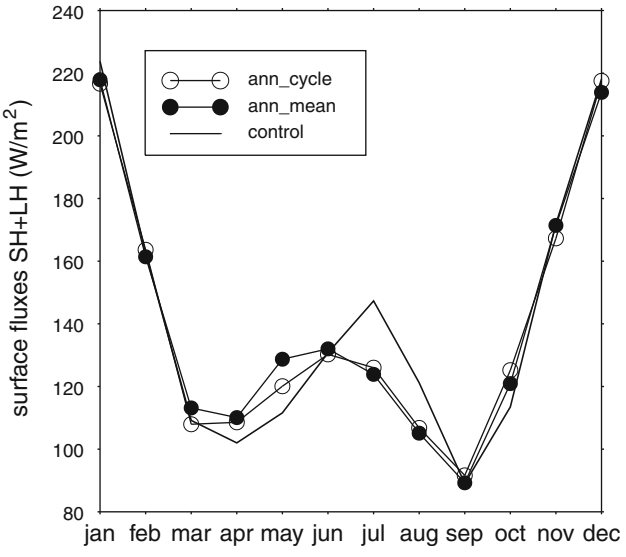

Fig. 9 Mean seasonal cycle of turbulent surface fluxes (sum of latent and sensible heat) in *ann_mean* (*solid circle*) and *ann_cycle* (*white circle*) SeaWiFS-forced integrations and the global chlorophyll control integration (*solid*) over the 58−62°E, 15−18°N region. Units are Wm^{-2} and positive represents upwards fluxes

summer, unlike autumn as in Wetzel et al. (2006). This may relate to slight differences in the region of study or our prescription of accurate observed chlorophyll concentrations here compared to those produced by un-coupled biogeochemical modelling. While we have found that inclusion of this physical process has partially ameliorated biases in the seasonal cycle of the Arabian Sea, it is clear from Fig. 8 that substantial problems remain. These perhaps relate to other factors such as cold dry air advection from Pakistan and northwest India during the boreal winter monsoon, leading to large latent heat flux errors in the region among the CMIP3 models (Marathayil et al. 2011). The seasonal radiative effects of atmospheric dust are also likely to be a key process over the Arabian Sea owing to transport from desert regions in central and eastern Africa, and more locally from north–west India.

To explain the behaviour of surface temperature in this region more clearly, in Fig. 9 we show the evolution of turbulent surface heat fluxes in the SeaWiFS perturbation experiments. These clearly show the seasonal cycle of surface fluxes to be brought forward, with increases during April and May and reductions in July and August in the SeaWiFS experiments. The stronger upward fluxes centred on May in the *ann_mean* experiment relative to *ann_cycle* help explain the negative tendency in *ann_mean* SST between May and June in Fig. 8.

We now focus on the impact of the SeaWiFS experiments on the mixed layer, which, so far, has been shown to undergo general shoaling. In Fig. 10 we show the seasonal cycle of mixed layer depth in the west–central Arabian Sea

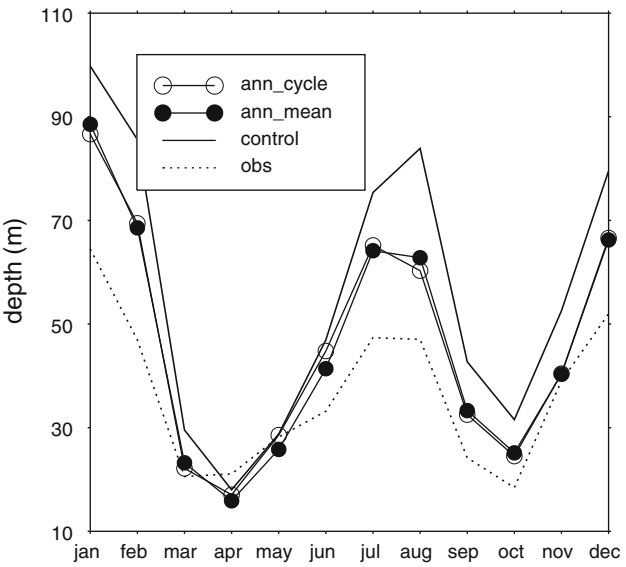

Fig. 10 Monthly climatological mixed layer depth in *ann_mean* (*solid circle*) and *ann_cycle* (*white circle*) SeaWiFS-forced integrations and the global chlorophyll control integration (*solid*) over the 58−62°E, 15−18°N region. Comparisons are made with an observed L'OCEAN climatology (*dotted*). Note that depth increases in the *upwards* direction on the *y* axis

in the SeaWiFS experiments compared with the L'OCEAN observed dataset. While there are clearly errors in the modelled mixed layer depth (it is too deep during boreal summer and winter) the pronounced seasonal cycle is captured. The SeaWiFS perturbation experiments go some way to overcoming the bias, reducing it by around 50%

during boreal summer. Given the size of the summer and winter biases, this comparison is unlikely to be affected by using an alternative algorithm for calculating the observed mixed layer depth climatology.

4.3 Discussion

We now turn to the apparent disparity between consistent mixed layer shoaling and differing changes in temperature at the sea surface outlined in the above experiments (e.g., comparing SST changes in June and July in Figs. 5, 7). We also show an example of changes in a winter case: Fig. 11 shows the MLD and SST changes during December in the SeaWiFS *ann_cycle* experiment. Unlike boreal summer, the prevailing wind direction is not conducive to coastal upwelling, yet the wind speed is strong. In December the deep mixed layer is shoaled by chlorophyll forcing, yet SST reduces over parts of the west central Arabian Sea. This cooling persists over substantial areas of the basin in January.

The discrepancy between consistent mixed layer shoaling and changes in SST of either sign in different months can be explained by the relative depth of the climatological mixed layer and penetration depth of anomalous incoming solar radiation. We explore this by examining the dominant contributions to ocean temperature tendencies as diagnosed by the GCM in case studies of the *ann_cycle* experiment. The cases chosen are: December, in which the mixed layer is deep and we have shown SST to decrease; April, in which the mixed layer is shallow and SST has increased; and July during the mature monsoon season, in which the mixed layer is again deep and the surface has cooled. Although the circumstances during December and July appear similar, they occur during winter monsoon (coastal downwelling) and summer monsoon (coastal upwelling) regimes respectively. In Fig. 12 we show the contributions in the top 100 m in the global chlorophyll control experiment (*chl_control*): from penetrating solar radiation (dT/dt_{SW}); from a combination of mixing processes and surface fluxes (dT/dt_{MLSF}); and the sum of other terms such as advection, diffusion and convection. The difference in these tendencies between the *ann_cycle* and *chl_control* experiments is also shown in the lower panels.

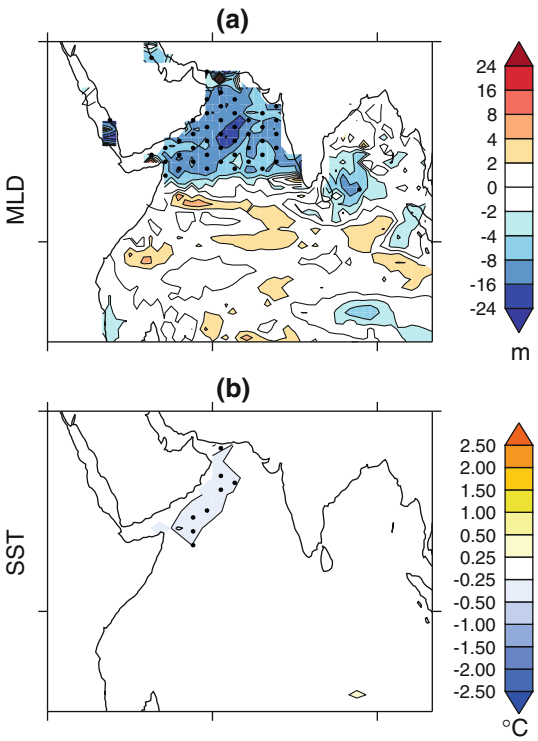

Fig. 11 Composite differences between the seasonally varying SeaWiFS experiment (*ann_cycle*) and fixed global chlorophyll control integration (*chl_control*) in December for mixed layer depth (**a**) and SST (**b**). Units are m and °C respectively. Differences statistically significant above the 95% level are shown by *solid stipples*

During December, strong winter monsoon winds and surface fluxes act to cool the surface maintaining a deep mixed layer (Fig. 12a). Near the surface, attenuation caused by chlorophyll suggests a warming tendency (red curve in Fig. 12d) however beneath this there is a negative tendency since the chlorophyll causes a shadow beneath it. The climatological mixed layer extends far beneath the depth to which solar radiation perturbs the ocean temperature (even following the significant mixed layer shoaling due to stabilization of the vertical temperature profile), encompassing also the negative tendency in the shadow region. Thus following mixing processes there is no net warming of the surface due to chlorophyll. In fact, the net surface cooling at this time of year forced by strong wind-driven evaporation means that these upward fluxes of heat now act on a more shallow mixed layer of lower heat capacity. This enhanced cooling tendency leads to anomalously large negative surface temperature perturbations as indicated in Figs. 12d (black curve) and 11b. The green curve in Fig. 12d also shows clear evidence of mixing processes at work, which act to cool the near surface layers while warming the lower part of the mixed layer. Thus chlorophyll has not acted to change the surface temperature directly but its stabilizing impact on the vertical temperature profile shoals the mixed layer and reduces the heat capacity, exacerbating the climatological surface cooling in December. We note that other processes including advection play a negligible role in temperature tendencies during December.

During April, winds are weak, the mixed layer is shallow and the surface undergoes net warming. The additional ocean temperature increment due to solar fluxes (dT/dt_{SW}) caused by the high chlorophyll concentration is encompassed entirely within the mixed layer, above the diagnosed

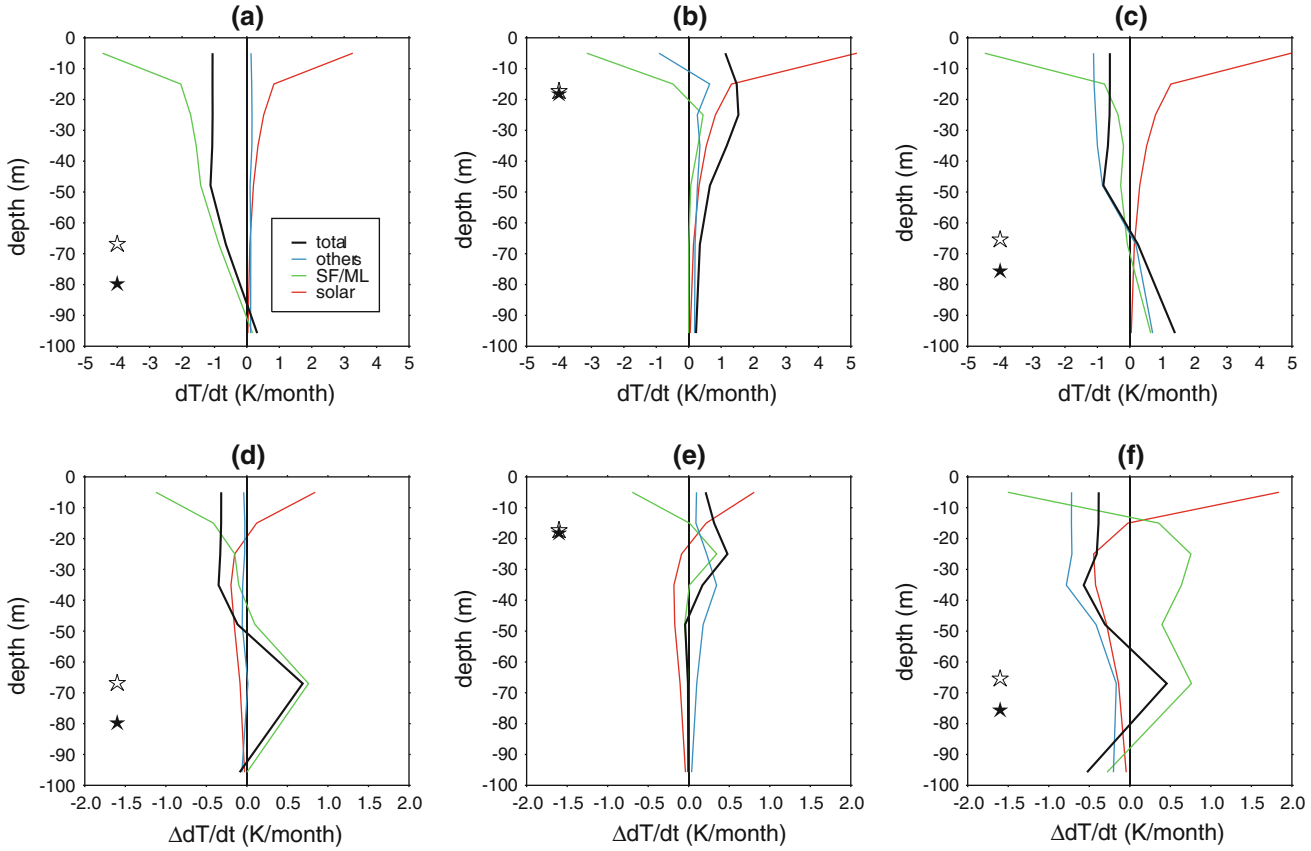

Fig. 12 Monthly temperature tendencies during **a**) December (**b**) April and (**c**) July caused by penetrative solar fluxes (termed dT/dt_{SW} in the *text*), a combination of surface fluxes and mixing (dT/dt_{MLSF}) and the sum of all other processes (advection, diffusion and convection) in the global chlorophyll control integration (*chl_control*). The total tendency is shown by the *thick black line*. Averaging is performed over the 58−62°E, 15−18°N region as in other figures. The perturbations to these tendencies in the *ann_cycle* SeaWiFS experiment are also shown for (**d**) December, (**e**) April and (**f**) July. Units are °C/month. Each *panel* also shows the mean mixed layer depth in *chl_control* (*ann_cycle*) experiments as a *solid* (*empty*) *star*

MLD. The mixed layer is shoaled only partially in the east (Fig. 7b). Less radiation penetrates beneath the chlorophyll in its shadow (see the red curve below ∼20 m in Fig. 12e; also noted in Nakamoto et al. 2000). However since this is isolated from the mixed layer it does not affect SST. Rather than a heat capacity effect as in December, the solar term acts to enhance the total positive temperature tendency in this part of the season, ultimately leading to warmer SST in April. In the mixed layer, there is also a positive contribution from horizontal advection, balanced by a smaller increase in cooling from vertical advection (sum shown by the light blue curve in Fig. 12e).

In July the monsoon is well underway and its strong winds have already acted to deepen the mixed layer substantially. As in December, both the additional near-surface warming caused by the chlorophyll and the cooling beneath this are encompassed within the mixed layer (red curve in Fig. 12f). The near-surface warming perturbation from solar fluxes acts to stabilize the profile, shoaling the mixed layer slightly. Thus the net cooling tendencies at this time of year act on a reduced heat capacity, resulting in enhanced cooling of SST. This occurs despite the high chlorophyll concentration and contribution from solar radiation near the surface. Unlike December, coastal upwelling is a key feature of July's surface heat budget. The net effect of vertical over horizontal advection in July thus brings a significant negative contribution to near-surface temperatures.

Thus during periods of seasonally deep mixing (once the monsoons are well established) increased chlorophyll concentrations act to increase the surface cooling tendency and lead to colder SST. We note that the deep mixed layer bias of HadCM3 is not large enough to affect this result for enhanced surface cooling in December and July since the changes to the vertical temperature profile caused by chlorophyll would still be entirely encompassed within the layer itself.

In summary, additional SST warming due to chlorophyll occurs only during the equinoctial periods of shallow mixed layers, and thus can only yield positive impacts on

monsoon rainfall during the onset in the transition from spring to summer. The enhancement to climatological temperature tendencies at the surface, as shown for December, April and July cases, acts to strengthen the seasonal cycle of SST in the Arabian Sea.

5 Conclusions

In this study we have examined the effect of changing the solar absorption properties in the Arabian Sea region on its climate and that of the South Asian summer monsoon. This is motivated by the large seasonal cycle of chlorophyll in the region, which is partly forced by rapid deepening of the mixed layer as the seasonal monsoon winds develop (Lévy et al. 2007).

A high spatial and temporal resolution chlorophyll climatology generated for the Indian Ocean by Lévy et al. (2007) from SeaWiFS retrievals has been used to supply a seasonal cycle of concentrations to the ocean model. These concentrations are converted directly to penetration length scales appropriate for the two-band radiation scheme in the upper ocean following Ohlmann (2003). In these experiments, in which the high spatial inhomogeneity of the dataset is captured across the Arabian Sea despite the 1.25° horizontal resolution, we have shown clear evidence that the increased stability of the upper ocean shoals the mixed layer, significantly warming SST in late spring. This leads to additional westerly moisture advection incident upon peninsular India, and significant increases in precipitation during the onset of up to 2.5 mm/day. Such increases partially reduce the weak precipitation bias of this model during the onset noted in other work (Annamalai et al. 2007; Turner and Slingo 2009). Unlike the study of Wetzel et al. (2006) in which consistent increases were noted in precipitation over coastal India from July to September, the SST cooling in July and August in this study restricts the flow of moisture available to the monsoon in those months. As Wetzel et al. (2006) acknowledge, other studies including Nakamoto et al. (2000) also showed slight cooling from July to August. Thus incorporating atmospheric feedbacks, as we do here, leads to a complex response of the monsoon through the season.

Unlike the SST warming in late boreal spring, during strong monsoon wind regimes in July and December, SST is reduced by the inclusion of chlorophyll. Thus there is clear evidence that chlorophyll processes play an important role in the seasonality of the Arabian Sea, which supports the earlier results of Nakamoto et al. (2000) using only a forced OGCM. The seasonality and bias in mixed layer depth are also significantly improved, and we note that the deep mixed layer bias in HadCM3 is not large enough to alter the differing effects of chlorophyll on surface cooling or warming. (The reduced solar penetration in the shadow beneath the chlorophyll layer will still occur either above or below the base of the layer in December/July and April respectively). Other studies such as Marathayil et al. (2011) show the prevalence of large cold biases in the northern Arabian Sea during boreal winter and spring among the CMIP3 models. Rather than chlorophyll processes, other sources are clearly implicated in such biases (e.g., cold dry air advection from the north as in Marathayil et al. 2011). Levine and Turner (2011) have already shown such coupled model SST biases to have clear and significant impacts on monsoon precipitation, thus addressing them should be given a clear priority in order to improve dynamical seasonal prediction and long term climate projections of the South Asian summer monsoon.

This study has not considered the effect of seasonally varying chlorophyll in other regions. The Arabian Sea was chosen as a focus region because of the large magnitude of chlorophyll variability relative to that elsewhere in the Indian Ocean (see Fig. 2), and because of its proximity to the major centres of convection of the South Asian summer monsoon. Further experiments have been carried out in which the seasonal cycle of SeaWiFS chlorophyll constructed from the Lévy et al. (2007) data is prescribed over the whole Indian Ocean. In these experiments very similar results are found for the SST changes in the Arabian Sea and redistribution of moisture during the monsoon, further strengthening the case for inclusion of chlorophyll variability in coupled GCMs.

This study has also not evaluated the potential impact on variability in the Arabian Sea and thus the monsoon. The overly deep mixed layer in HadCM3 may restrict variability in SST and moisture over the Arabian Sea on intraseasonal timescales. The once per day atmosphere-ocean coupling frequency used in this model and in many other state-of-the-art CMIP3 GCMs will also inhibit diurnal variability in the mixed layer and hence variability in both SST and chlorophyll production.

A further enhancement to this study could consider feedbacks on phytoplankton development by coupling with ocean biology models, although considerable uncertainties remain in their simulation of phytoplankton growth. Lévy et al. (2007) showed that the seasonal phytoplankton bloom was caused by rapid deepening of the mixed layer at the onset of the monsoon, thus inconsistencies between the timing of a prescribed chlorophyll bloom and that of the monsoon onset of the coupled GCM will cause errors in the SST response to chlorophyll. At the time of the monsoon onset, interannual variability in SeaWiFS-derived chlorophyll averaged over a broad region of the central Arabian Sea is at its lowest (around 10%, Robertson 2011). However in recent work using a 1D mixed layer model, Robertson (2011) found that this variability causes SST

changes of up to ±0.2 K over the Arabian Sea at this time. This gives an estimate of the error one might expect from inconsistencies between the timing of the bloom and the monsoon onset. Interannual variability of chlorophyll reaches almost as high as 35% between June and July, but its effect on SST variability is lower owing to the climatologically deep mixed layer. Realistic modelling of chlorophyll concentrations in the Arabian Sea might lead to better simulation of interannual variability in the monsoon and improved seasonal forecasts. The inclusion of such Earth System feedbacks in the latest high resolution coupled GCMs will eventually allow the effects of ocean chlorophyll on climate to be addressed in more detail.

Acknowledgments A. G. Turner is funded by a NERC Fellowship number NE/H015655/1; M. Joshi and S. J. Woolnough were funded by the National Centre for Atmospheric Science Climate directorate, a NERC collaborative centre. E. S. Robertson was funded under a NERC-tied studentship grant number NE/D010810/1. Computing resources for running the Hadley Centre model were provided by HECToR. The authors thank the two anonymous reviewers and the Editor, Susanna Corti, whose comments have helped to improve this manuscript.

References

Anderson W, Gnanadesikan A, Wittenberg A (2009) Regional impacts of ocean color on tropical Pacific variability. Ocean Sci Ocean Eng 5(3):313–327

Annamalai H, Hamilton K, Sperber KR (2007) The South Asian summer monsoon and its relationship with ENSO in the IPCC AR4 simulations. J Clim 20(6):1071–1092

Conkright ME, Gregg WW (2003) Comparison of global chlorophyll climatologies: In situ, CZCS, Blended in situ-CZCS and SeaWiFS. Int J Remote Sens 24(5):969–991

de Boyer Montégut CD, Madec G, Fischer AS, Lazar A, Iudicone D (2004) Mixed layer depth over the global ocean: an examination of profile data and a profile-based climatology. J Geophys Res Oceans 109(C12), C12003. doi:10.1029/2004JC002378

Desa E, Suresh T, Matondkar SGP (2001) Sea truth validation of SeaWiFS ocean colour sensor in the coastal waters of the Eastern Arabian Sea. Curr Sci 80(7):854–860

Foreman SJ (1990) Ocean model mixed layer formulation. Unified Model Documentation Paper 41, UK Met Office

Gnanadesikan A, Anderson WG (2009) Ocean water clarity and the ocean general circulation in a coupled climate model. J Phys Oceanogr 39(2):314–332

Gnanadesikan A, Emanuel K, Vecchi GA, Anderson WG, Hallberg R (2010) How ocean color can steer Pacific tropical cyclones. Geophys Res Lett 37, L18802. doi:10.1029/2010GL044514

Gordon C, Cooper C, Senior CA, Banks H, Gregory JM, Johns TC, Mitchell JFB, Wood RA (2000) The simulation of SST, sea ice extents and ocean heat transports in a version of the Hadley Centre coupled model without flux adjustments. Clim Dyn 16(2–3):147–168

Gregg WW, Casey NW (2004) Global and regional evaluation of the SeaWiFS chlorophyll data set. Remote Sens Environ 93(4):463–479

Gregg WW, Casey NW (2007) Sampling biases in MODIS and SeaWiFS ocean chlorophyll data. Remote Sens Environ 111(1):25–35

Izumo T, de Boyer Montégut CD, Luo JJ, Behera SK, Masson S, Yamagata T (2008) The role of the Western Arabian Sea upwelling in Indian monsoon rainfall variability. J Clim 21(21): 5603–5623

Jerlov NG (1968) Optical oceanography. Elsevier, Amsterdam

Ju JH, Slingo J (1995) The Asian Summer Monsoon and ENSO. Q J Roy Meteorol Soc 121(525):1133–1168

Kraus EB, Turner JS (1967) A one dimensional model of the seasonal thermocline. Part II. The general theory and its consequences. Tellus 19(1):98–106. doi:10.1111/j.2153-3490.1967.tb01462.x

Krishnan R, C Z, Sugi M (2000) Dynamics of breaks in the Indian summer monsoon. J Atmospheric Sci 57:1354–1372

Lengaigne M, Menkes C, Aumont O, Gorgues T, Bopp L, Andre JM, Madec G (2007) Influence of the oceanic biology on the tropical Pacific climate in a coupled general circulation model. Clim Dyn 28(5):503–516

Levine RC, Turner AG (2011) Dependence of Indian monsoon rainfall on moisture fluxes across the Arabian Sea and the impact of coupled model sea surface temperature biases. Clim Dyn. doi: 10.1007/s00382-011-1096-z

Lévy M, Shankar D, Andre JM, Shenoi SSC, Durand F, de Boyer Montégut C (2007) Basin-wide seasonal evolution of the Indian Ocean's phytoplankton blooms. J Geophys Res Oceans 112(C12), C12014. doi:10.1029/2007JC004090

Lin PF, Liu HL, Mang XH (2007) Sensitivity of the upper ocean temperature and circulation in the equatorial Pacific to solar radiation penetration due to phytoplankton. Adv Atmos Sci 24:765–780

Marathayil D, Shaffrey LC, Turner AG (2011) Examination of Arabian Sea SST biases in the HiGEM high resolution coupled climate model and the CMIP3 multi-model dataset. Geophys Res Lett (in preparation)

Meehl GA, Covey C, Delworth T, Latif M, McAveney B, Mitchell JFB, Stouffer RJ, Taylor KE (2007) The WCRP CMIP3 multi-model dataset: a new era in climate change research. Bull Am Meteorol Soc 88:1383–1394

Nakamoto S, Kumar SP, Oberhuber JM, Muneyama K, Frouin R (2000) Chlorophyll modulation of sea surface temperature in the Arabian Sea in a mixed-layer isopycnal general circulation model. Geophys Res Lett 27(6):747–750

Nakamoto S, Kumar SP, Oberhuber JM, Ishizaka J, Muneyama K, Frouin R (2001) Response of the equatorial Pacific to chlorophyll pigment in a mixed layer isopycnal ocean general circulation model. Geophys Res Lett 28(10):2021–2024

Ohlmann JC (2003) Ocean radiant heating in climate models. J Clim 16(9):1337–1351

Parthasarathy B, Munot AA, Kothawale DR (1994) All-India Monthly and Seasonal Rainfall Series—1871–1993. Theor Appl Climatol 49(4):217–224

Paulson CA, Simpson JJ (1977) Irradiance measurements in upper ocean. J Phys Oceanogr 7(6):952–956

Pope VD, Gallani ML, Rowntree PR, Stratton RA (2000) The impact of new physical parametrizations in the Hadley Centre climate model: HadAM3. Clim Dyn 16(2–3):123–146

Rajeevan M, Bhate J, Kale JD, Lal B (2006) High resolution daily gridded rainfall data for the Indian region: Analysis of break and active monsoon spells. Curr Sci 91:296–306

Rayner NA, Parker DE, Horton EB, Folland CK, Alexander LV, Rowell DP, Kent EC, Kaplan A (2003) Global analyses of sea surface temperature, sea ice, and night marine air temperature since the late nineteenth century. J Geophys Res Atmospheres 108(D14), 4407. doi:10.1029/2002JD002670

Robertson ES (2011) Biophysical coupling in the ocean mixed layer. Ph.D. thesis, submitted, Department of Meteorology, University of Reading

Sathyendranath S, Gouveia AD, Shetye SR, Ravindran P, Platt T (1991) Biological-control of surface-temperature in the Arabian Sea. Nat Biotechnol 349(6304):54–56

Schott FA, McCreary JP (2001) The monsoon circulation of the Indian Ocean. Prog Oceanogr 51(1):1–123

Shell KM, Frouin R, Nakamoto S, Somerville RCJ (2003) Atmospheric response to solar radiation absorbed by phytoplankton. J Geophys Res Atmospheres 108(D15), 4445. doi:10.1029/2003JD003440

Slingo J, Spencer H, Hoskins B, Berrisford P, Black E (2005) The meteorology of the Western Indian Ocean, and the influence of the east African highlands. Phil Trans Roy Soc A—Math Phys Eng Sci 363(1826):25–42

Turner AG, Slingo JM (2009) Subseasonal extremes of precipitation and active-break cycles of the Indian summer monsoon in a climate-change scenario. Q J Roy Meteorol Soc 135(640): 549–567

Turner AG, Inness PM, Slingo JM (2005) The role of the basic state in the ENSO-monsoon relationship and implications for predictability. Q J Roy Meteorol Soc 131(607):781–804

Turner AG, Inness PA, Slingo JM (2007) The effect of doubled CO2 and model basic state biases on the monsoon-ENSO system. I: Mean response and interannual variability. Q J Roy Meteorol Soc 133(626):1143–1157

Uppala SM, Kallberg PW, Simmons AJ, Andrae U, Bechtold VD, Fiorino M, Gibson JK, Haseler J, Hernandez A, Kelly GA, Li X, Onogi K, Saarinen S, Sokka N, Allan RP, Andersson E, Arpe K, Balmaseda MA, Beljaars ACM, Van De Berg L, Bidlot J, Bormann N, Caires S, Chevallier F, Dethof A, Dragosavac M, Fisher M, Fuentes M, Hagemann S, Holm E, Hoskins BJ, Isaksen L, Janssen P, Jenne R, McNally AP, Mahfouf JF, Morcrette JJ, Rayner NA, Saunders RW, Simon P, Sterl A, Trenberth KE, Untch A, Vasiljevic D, Viterbo P, Woollen J (2005) The ERA-40 re-analysis. Q J Roy Meteorol Soc 131(612):2961–3012 Part B

Vecchi GA, Harrison DE (2004) Interannual Indian rainfall variability and Indian ocean sea surface temperature anomalies. In: Wang C, Xie SP, Carton JA (eds), Earth's Climate: the Ocean-Atmosphere Interaction. AGU Monograph, vol 147, pp 247–259. Conference on Ocean-Atmosphere Interaction and Climate Variability, December 2002, San Francisco, CA

Wetzel P, Maier-Reimer E, Botzet M, Jungclaus J, Keenlyside N, Latif M (2006) Effects of ocean biology on the penetrative radiation in a coupled climate model. J Clim 19(16):3973–3987